Theoretical Compton profile anisotropies in molecules and solids. IV. Parallel–perpendicular anisotropies in alkali fluoride molecules

Robert L. Matcha, Bernard M. Pettitt, B. I. Ramirez, and William R. McIntire

Citation: The Journal of Chemical Physics **71**, 991 (1979); doi: 10.1063/1.438390
View online: http://dx.doi.org/10.1063/1.438390
View Table of Contents: http://scitation.aip.org/content/aip/journal/jcp/71/2?ver=pdfcov
Published by the AIP Publishing

Theoretical Compton profile anisotropies in molecules and solids. IV. Parallel–perpendicular anisotropies in alkali fluoride molecules

Robert L. Matcha and Bernard M. Pettitt

Department of Chemistry, University of Houston, Houston, Texas 77004

B. I. Ramirez

Department of Physics, University of the Phillippines, Oilman, Quezon City, Phillippines

William R. McIntire

Chemical Engineering Division, Argonne National Laboratory, Argonne, Illinois 60439
(Received 27 April 1978)

Calculations of Compton profiles and parallel–perpendicular anisotropies in alkali fluorides are presented and analyzed in terms of molecular charge distributions and wave function character. It is found that the parallel profile associated with the valence pi orbital is the principal factor determining the relative shapes of the total profile anisotropies in the low momentum region.

I. INTRODUCTION

In this series of papers we are presenting a general study of crystalline and diatomic Compton profiles and their anisotropies. In this paper we examine the relationship between charge distributions in single bonds and Compton profile anisotropies associated with scattering vectors parallel and perpendicular to the bond axes in alkali fluoride molecules. Similar calculations on the alkali chlorides were presented in a previous paper. Our overall aim is to determine to what extent it is possible to extract useful chemical information from profile anisotropies. The Compton profiles are computed from first principles using SCF-LCAO-MO wavefunctions[1] in conjunction with the formalism developed[2] in I.

II. TOTAL COMPTON PROFILES

Parallel and perpendicular Compton profiles, $J_0(p_z')$, and $J_{90}(p_z')$, respectively, along with the isotropic profile $J_{av}(p_z')$ have been calculated at equilibrium diatomic spacings for LiF, NaF, KF, and RbF and tabulated in Table I. A resolution of J_0 and J_{90} into sigma and pi molecular orbital components for KF is given in Figs. 1–4. The profiles associated with fluorine AO's have shapes similar to corresponding LiF profiles illustrated

TABLE I. Selected values of J_{av}, J_{90} for LiF, NaF, KF, RbF all at R_e.

	LiF			NaF			KF			RbF		
p_z	J_{av}	J_0	J_{90}	J_{av}	J_0	J_{90}	J_{av}	J_0	J_{90}	J_{av}	J_0	J_{90}
0.0	3.9914	4.0951	3.9649	5.6302	5.5883	5.6364	7.7063	7.5922	7.7448	9.8042	9.6700	9.8669
0.1	3.9713	4.0546	3.9526	5.6116	5.5695	5.6222	7.6741	7.5615	7.7223	9.7665	9.6444	9.8343
0.2	3.9105	3.9427	3.9141	5.5521	5.5095	5.5730	7.5771	7.4787	7.6458	9.6484	9.5601	9.7273
0.3	3.8084	3.7810	3.8342	5.4440	5.1402	5.4753	7.4107	7.3463	7.4961	9.4386	9.3924	9.5263
0.4	3.6660	3.5914	3.7057	5.2833	5.2416	5.3207	7.1692	7.1409	7.2586	9.1319	9.1144	9.2190
0.5	3.4878	3.3897	3.5297	5.0739	5.0361	5.1117	6.8549	6.8435	6.9340	8.7378	8.7237	8.8095
0.6	3.2815	3.1852	3.3149	4.8265	4.7966	4.8588	6.4805	6.4653	6.5367	8.2753	8.2490	8.3160
0.7	3.0558	2.9809	3.0745	4.5540	4.5364	4.5760	6.0641	6.0402	6.0883	7.7651	7.7319	7.7648
0.8	2.8197	2.7771	2.8216	4.2681	4.2667	4.2767	5.6231	5.6024	5.6113	7.2262	7.2065	7.1849
0.9	2.5806	2.5728	2.5675	3.9778	3.9944	3.9721	5.1716	5.1725	5.1268	6.6769	6.6908	6.6046
1.0	2.3449	2.3678	2.3211	3.6893	3.7232	3.6709	4.7214	4.7559	4.6521	6.1350	6.1900	6.0473
1.2	1.9036	1.9622	1.8724	3.1344	3.1903	3.1014	3.8631	3.9545	3.7821	5.1381	5.2396	5.0646
1.4	1.5221	1.5817	1.4980	2.6276	2.6810	2.5969	3.1147	3.2025	3.0618	4.3301	4.4022	4.2981
1.6	1.2101	1.2491	1.1983	2.1843	2.2163	2.1664	2.5170	2.5573	2.5008	3.7345	3.7503	3.7338
1.8	0.9647	0.9773	0.9639	1.8118	1.8175	1.8079	2.0730	2.0686	2.0791	3.3162	3.3006	3.3252
2.0	0.7767	0.7679	0.7824	1.5088	1.4951	1.5142	1.7561	1.7331	1.7666	3.0178	3.0018	3.0237
2.5	0.4834	0.4625	0.4894	0.9963	0.9791	1.0015	1.2887	1.2849	1.2867	2.5163	2.5167	2.5142
3.0	0.3306	0.3284	0.3309	0.7011	0.7046	0.6990	1.0237	1.0281	1.0218	2.1428	2.1441	2.1420
3.5	0.2402	0.2469	0.2390	0.5159	0.5244	0.5140	0.8423	0.8454	0.8425	1.8186	1.8251	1.8181
4.0	0.1816	0.1839	0.1811	0.3943	0.3943	0.3942	0.7025	0.7031	0.7026	1.5304	1.5283	1.5304
4.5	0.1417	0.1398	0.1417	0.3117	0.3084	0.3117	0.5872	0.5855	0.5872	1.2826	1.2815	1.2827
5.0	0.1133	0.1120	0.1133	0.2522	0.2532	0.2519	0.4909	0.4915	0.4907	1.0762	1.0783	1.0763
5.5	0.0918	0.0924	0.0917	0.2068	0.2091	0.2066	0.4107	0.4122	0.4105	0.9081	0.9075	0.9082
6.0	0.0750	0.0757	0.0749	0.1713	0.1708	0.1711	0.3444	0.3437	0.3441	0.7727	0.7721	0.7727

 0021-9606/79/020991-06$01.00

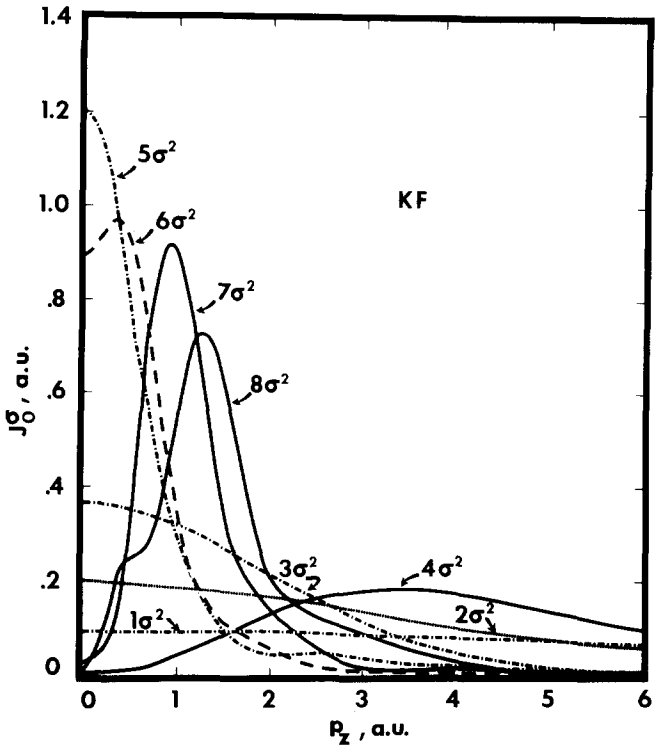

FIG. 1. Resolution of J_0 into sigma molecular orbital components for KF at $Re = 4.1035$.

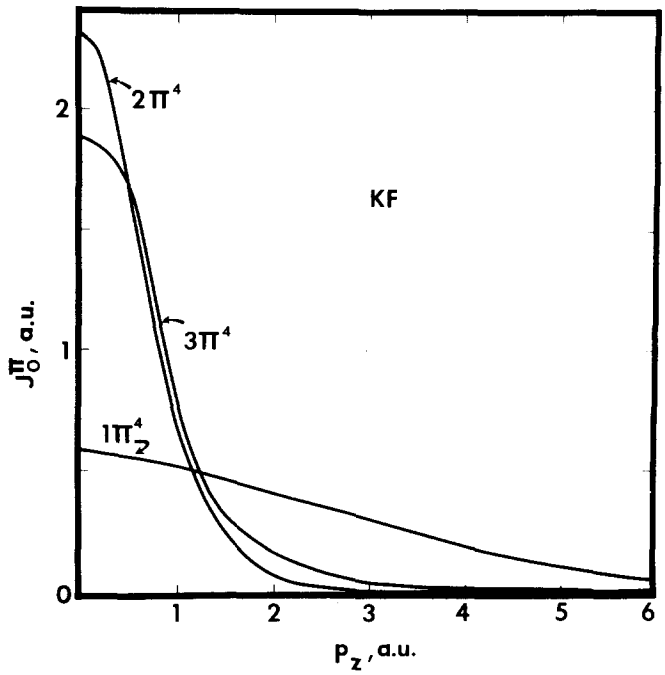

FIG. 3. Resolution of J_0 into pi molecular orbital components for KF at $Re = 4.1035$.

in Ref. 3. The main difference from molecule to molecule is the location and magnitude of local minima and maxima.

The $J_0^{n\sigma}$ and $J_{90}^{n\sigma}$ profiles ($n = 1, 8$) are illustrated in Figs. 1 and 2, respectively. The $1\sigma(1s_K)$, $2\sigma(1s_F)$ and $3\sigma(2s_K)$ MO's have characteristic s atomic orbital profiles.[3] They have maximum values at the origin and decrease asymptotically to zero. The extended nature of the inner shell profiles reflect the fact that the corresponding charge densities are highly localized. The $5\sigma(3s_K)$ profiles have the general features characteristic of s-orbitals. However $J_0^{5\sigma}$ has a local minimum of 0.0407 at 2.2 and local maximum of 0.04212 at 2.5 while $J_{90}^{5\sigma}$ has a plateau at 2.3 with value 0.04137. This structure is related to the nodal character of the 5σ MO.

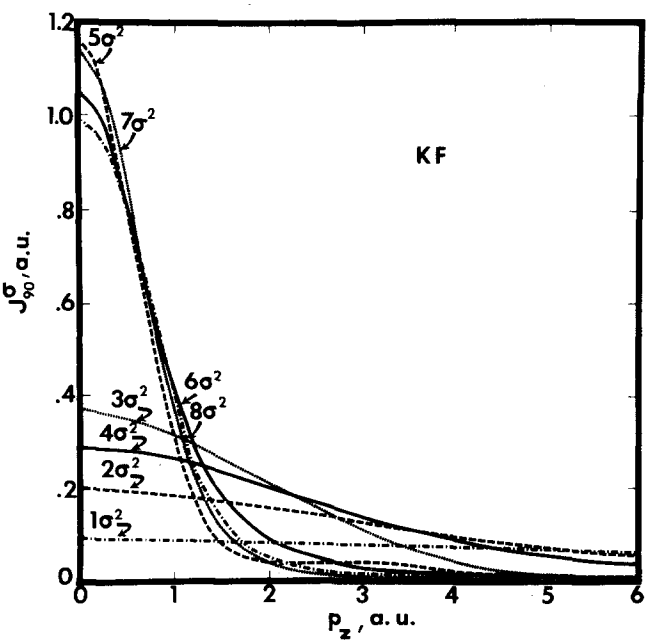

FIG. 2. Resolution of J_{90} into sigma molecular orbital components for KF at $Re = 4.1035$.

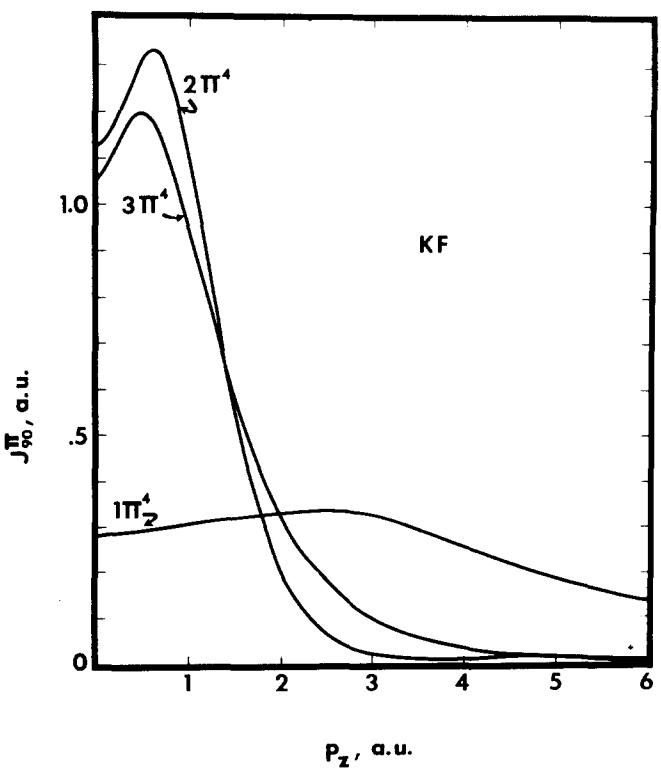

FIG. 4. Resolution of J_{90} into pi molecular orbital components for KF at $Re = 4.1035$.

The $4\sigma(2p_K)$, $7\sigma(3p_K)$ and $8\sigma(2p_F)$ $J_0^{n\sigma}$ profiles are characteristic of $p\sigma$ profiles. They rise initially from zero at the origin, reach a maximum and decrease asymptotically to zero. The corresponding $J_{90}^{n\sigma}$ profiles are maximum at the origin and asymptotically decrease to zero.

Interestingly, the maxima and minima in $n\sigma$ profiles are observed only in $J_0^{n\sigma}$ components. Plateaus, at most, are observed in the $J_{90}^{n\sigma}$ profiles. The opposite behavior is found in the $J_0^{n\pi}$ and $J_{90}^{n\pi}$ profiles. In this case it is only the latter that exhibit structure. In Figs. 3 and 4 we plot pi orbital contributions to the potassium fluoride parallel and perpendicular profiles. These are typical of $2p_\pi$ orbitals. The $1\pi(2p_K)$ and $3\pi(2p_F)$ profiles exhibit no fine structure in the range of p_z from zero to six. The $2\pi(3p_K)$ component, $J_{90}^{2\pi}$, has a minimum at 3.6 from 0.0149 and a maximum of 0.0167 at 4.6.

The isotropic profiles J_{av} given in Table I are illustrated in Fig. 5 where we plot J_{av} as a function of p_z for the fluorides (solid lines). These have been computed at the equilibrium diatomic spacings. Included are experimental and computed profiles (long dashed lines)

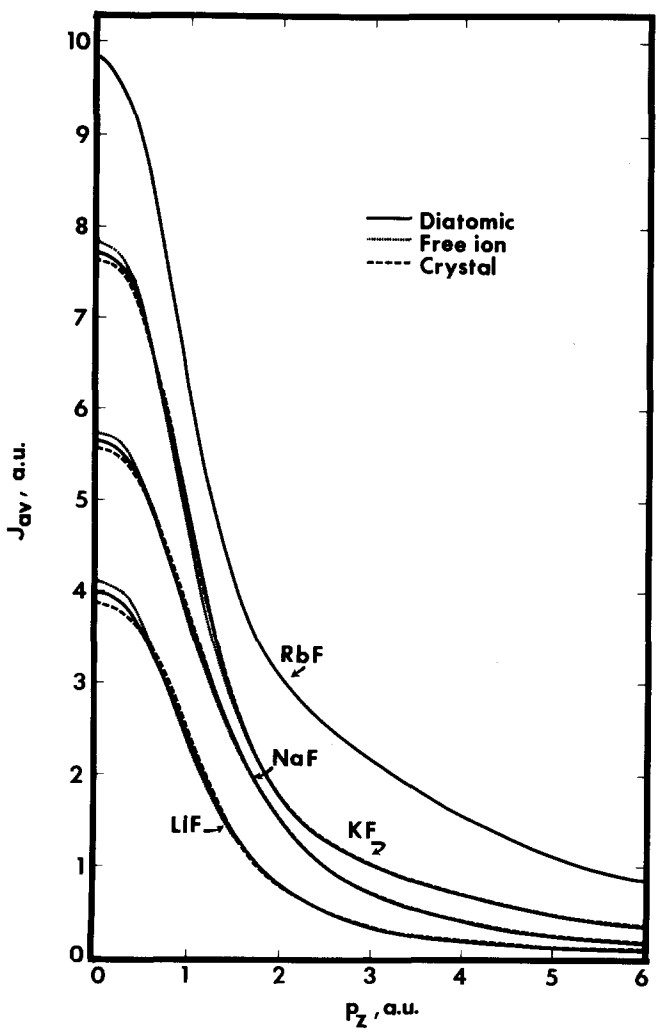

FIG. 5. Computed free ion and diatomic angle averaged Compton profiles along with experimental crystalline values for alkali fluorides.

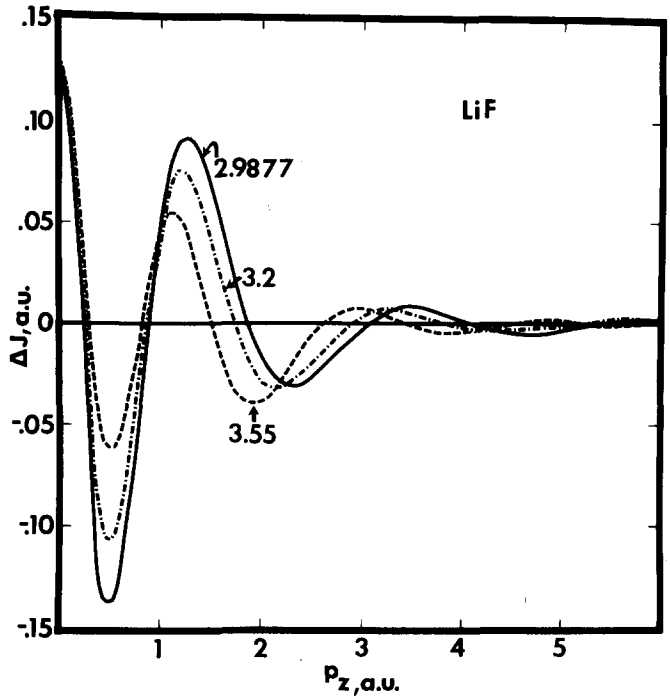

FIG. 6. Total Compton profile anisotropies for LiF at several spacings.

and free ion profiles computed in the Hartree-Fock approximation by Paakari *et al.*[4] (short dashed lines). Notice that the zero point Compton profiles decrease in the sequence free ion, diatomic and crystal reflecting increasing charge localization and momentum delocalization associated with bond formation. The long range momentum distributions are associated primarily with inner shell orbitals. It can be seen that the computed and experimental profiles agree for large p_z.

Normalizing the curves in Fig. 5 to one electron yields a new set of curves with the one dimensional probabilities at zero momentum decreasing in the sequence LiF, NaF, KF, and RbF. This reflects tighter binding in the alkali ion inner shells.

III. COMPTON PROFILE ANISOTROPIES

Although the isotropic profiles exhibit, to some degree, patterns characteristic of chemical bonds, they have limited information content. Intrinsically more informative are the difference profiles $\Delta J = J_0 - J_{90}$. Consider, for example in Figs. 6, 7, 8, and 9 where we plot the Compton profile anisotropies computed using data in Table I for LiF, KF, NaF, and RbF (Solid lines).

In Fig. 7 a partial resolution of the KF profile anisotropy into outer orbital contributions is illustrated. It can be seen that the total anisotropy is largely a reflection of the anisotropy associated with the valence $8\sigma(2p_F)$ and $3\pi(2p_F)$ MO's. This anisotropy is given by the sum $\Delta J^{8\sigma} + \Delta J^{3\pi}$ and reflects, primarily, via a complimentary relationship, distortions of the valence $2p_F^\sigma$ atomic orbital charge density associated with bond formation.

Insight into the genesis of the total anisotropies can be obtained by examining contributions from each molecular orbital to zero point (i.e., $p_z = 0$) profiles and

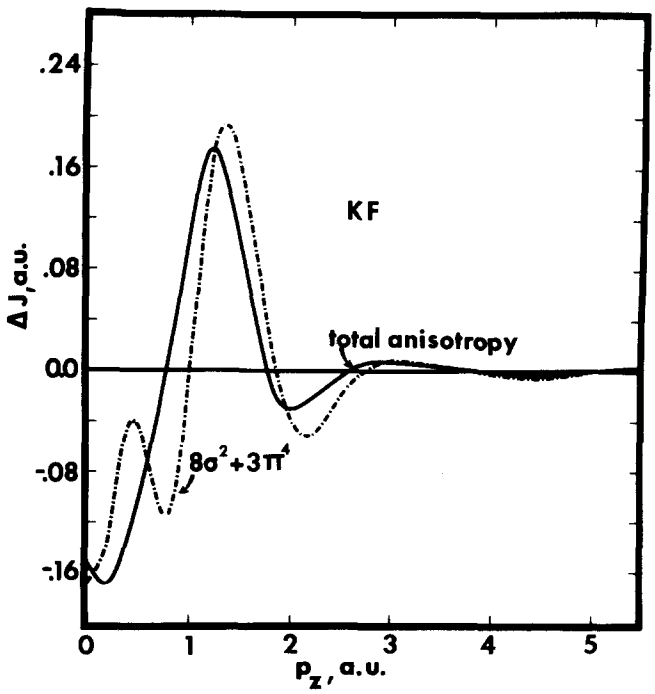

FIG. 7. Total and valence component Compton profile anisotropies for KF at $Re = 4.1035$.

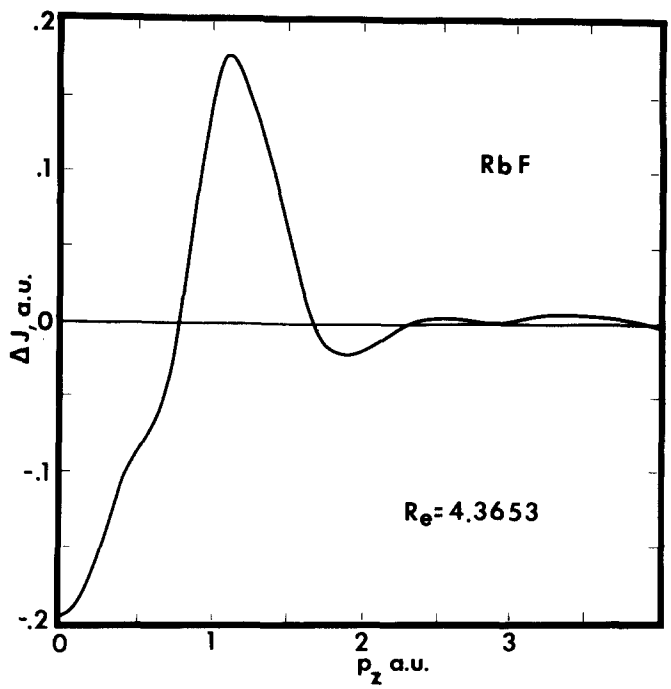

FIG. 9. Total Compton profile anisotropy for RbF at $Re = 4.3653$.

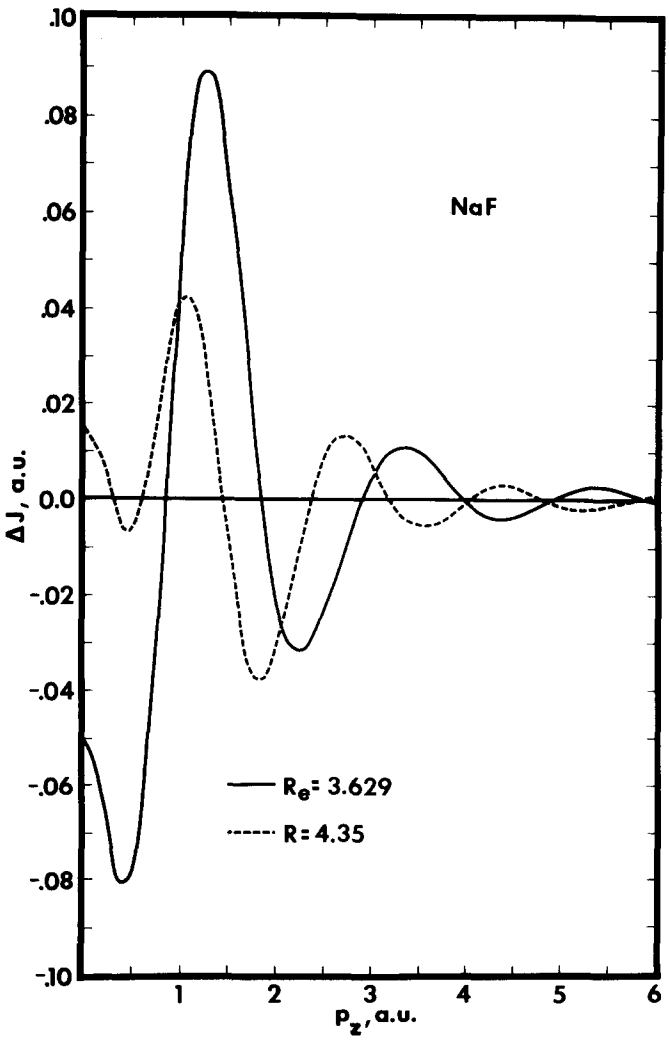

FIG. 8. Total Compton profile anisotropies for NaF at $R = 4.35$ and $Re = 3.629$.

anisotropies. In Table II we tabulate $J_0(0)$, $J_{90}(0)$, and $J_{av}(0)$ for the fluorides computed at several values of R. Consider first zero-point MO contributions to KF profiles computed at Re. The first three MO's, 1σ, 2σ, and 3σ, correspond to atomic s functions. No anisotropies are evident in these. The 4σ and 1π MO's are $2p_K$ AO's. Anisotropies associated with these sum to zero. Since these inner shell MO's do not contribute to the anisotropy they are not listed in the table.

The zero point $6\sigma(2s_F)$ anisotropy is quite large (-0.145). This reflects a relatively low value, 0.907, for $J_0^{6\sigma}(0)$. This quantity is a measure of the probability of finding electrons moving normal to the bond axis in the 6σ MO. The contribution to ΔJ from the 6σ MO tends to cancel contributions from the 5σ and sum of 7σ and 2π MO's.

It was found in the case of alkali chlorides[5] that the sum $\Delta J^{v\sigma}(0) + \Delta J^{v\pi}(0)$ contributes substantially to the zero point anisotropy (v here refers to valence). This is also true of the alkali fluorides. An examination of the column headed by ΔJ in Table II indicates that the sum of the valence sigma and pi contributions to LiF, NaF, KF, and RbF anisotropies equals 0.1961, -0.0269, -0.1721, and -0.2080, respectively at Re. The corresponding zero point anisotropies are 0.1302, -0.0481, -0.1525, and -0.1952. Furthermore, most of the variation in $\Delta J(0)$ can be associated with $J_0^{v\pi}(0)$ through the series. If we assign average values of $J_0^{v\sigma}(0) \approx 0.01$, $J_{90}^{v\sigma}(0) \approx 0.98$, and $J_{90}^{v\pi}(0) \approx 1.06$ we obtain the approximate formula $\Delta J(0) \approx -2.05 + J_0^{v\pi}$ for the fluorides. This yields zero point anisotropies of 0.199, 0.070, -0.153, and -0.223 for LiF, NaF, KF, and RbF, respectively. This suggests that polarization or overlapping of valence $p\pi$ orbitals with attendent charge buildup in the bonding region (factors which decrease probabilities of electrons

TABLE II. Resolution of zero point Compton profile anisotropies for LiF, NaF, KF, and RbF. The LiF, NaF, and KF values are computed at two different spacings.

Molecule	R[a]	Orbital i	$J_0^i(0)$	J_{90}^i	$\Delta J^i(0)$	Δ[b]
LiF	3.55(2.987)	$2\sigma^2(1s_{Li})$	0.6675(0.6889)[a]	0.6577(0.6601)	0.0098(0.0288)	0.0190
		$3\sigma^2(2s_F)$	1.0207(0.9531)	1.0470(1.0480)	−0.0263(−0.0949)	−0.0686
		$4\sigma_4(2p_F)$	0.0077(0.0196)	1.0362(0.9982)	−1.0285(−0.9786)	0.0499
		$1\pi^4(2p_F)$	2.2243(2.2327)	1.0489(1.0580)	1.1754(1.1747)	−0.0007
				$\Delta J(0)$	0.1304(0.1300)	−0.0004
NaF	4.35(3.629)	$3\sigma^2(2s_{Na})$	0.7806(0.7863)	0.7813(0.7822)	−0.0007(0.0041)	0.0048
		$4\sigma^2(2p_{Na})$	0.0012(0.0204)	0.6731(0.6878)	−0.6719(−0.6674)	0.0045
		$5\sigma^2(2s_F)$	1.0489(0.9988)	1.0523(1.0402)	−0.0034(−0.0414)	−0.0380
		$6\sigma^2(2p_F)$	0.0099(0.0073)	1.0618(1.0246)	−1.0519(−1.0173)	0.0346
		$1\pi^4(2p_{Na})$	1.3491(1.3584)	0.6736(0.6749)	0.6755(0.0835)	0.0080
		$2\pi^4(2p_F)$	2.1197(2.0534)	1.0541(1.0630)	1.0656(0.9904)	−0.0752
				$\Delta J(0)$	0.0132(−0.0481)	−0.0613
KF	4.8(4.1035)	$5\sigma^2(3s_K)$	1.1490(1.2033)	1.1442(1.1477)	0.0048(0.0556)	0.0508
		$6\sigma^2(2s_F)$	1.0243(0.9069)	1.0585(1.0518)	−0.0342(−0.1449)	−0.1107
		$7\sigma^2(3p_K)$	0.0071(0.0300)	1.1157(1.1218)	−1.1086(−1.0918)	0.0168
		$8\sigma^2(2p_F)$	0.0092(0.0034)	0.9847(0.9822)	−0.9755(−0.9788)	−0.0033
		$2\pi^4(3p_K)$	2.2846(2.3251)	1.1282(1.1348)	1.1564(1.1903)	0.0339
		$3\pi\ (2p_F)$	1.9400(1.8810)	1.0525(1.0643)	0.8875(0.8167)	−0.0708
				$\Delta J(0)$	−0.0696(−0.1529)	−0.0833
RbF	(4.3653)	$8\sigma_2^2(4s_{Rb})$	(1.4437)	(1.2910)	(0.1527)	
		$9\sigma^2(2s_F)$	(0.8066)	(1.0611)	(−0.2545)	
		$10\sigma^2(4p_{Rb})$	(0.0268)	(1.3193)	(−1.2925)	
		$11\sigma^2(2p_F)$	(0.0034)	(0.9857)	(−0.9823)	
		$4\pi^4(4p_{Rb})$	(2.7463)	(1.3363)	(1.4101)	
		$5\pi^4(2p_F)$	(1.8106)	(1.0363)	(0.7743)	
				$\Delta J(0)$	(−0.1923)	

[a]Values in parentheses are computed at Re.
[b]The quantity Δ is the change in $\Delta J^i(0)$ going from R to Re.

moving normal to the bond axis and increase probabilities of parallel motion) contribute substantially to the variations in $\Delta J(0)$ in the fluoride (as well as chloride) sequence.

IV. DEPENDENCE OF ANISOTROPIES ON INTERNUCLEAR DISTANCE

We next examine the manner which ΔJ varies with R for fluorides. In Figs. 6, 8, and 10, we plot ΔJ vs p_z for LiF, NaF, and KF computed at several values of R. The solid line refers to a calculation at Re. Certain trends are discernible. The curves in the range $0 < p_z < 1$ tend to become more negative as R decreases and more positive in the range $1 < p_z < 2$. Also the zero point change in ΔJ with R increases in the sequence LiF, NaF, and KF.

It is instructive to examine in some detail the changes in the molecular orbital contributions to the zero point profiles and anisotropies associated with varying R. Consider again Table II where we tabulate $J_0^i(0)$, $J_{90}^i(0)$, and $\Delta J^i(0)$ computed for LiF, NaF, and KF at two different values of R. For convenience, we include a quantity Δ representing the change in $\Delta J^i(0)$ going from R to Re. Two facts are evident: changes taking place in the sigma orbitals tend to cancel and the total zero point variation with R is approximately equal to the change occurring in the valence pi orbital. This is the same pattern observed in the chloride series.

Regarding the first point, a negative contribution to Δ from the MO correlating with the $2s_F$ AO is very nearly cancelled by the positive contributions from the sigma MO's correlating with the $2p_F$ AO and the nonvalence s and p AO's on the alkali ion. The latter two MO's are primarily anti bonding orbitals since the result of polarization by the negatively charged fluoride ion is to push charge out of the bonding region. To illustrate, con-

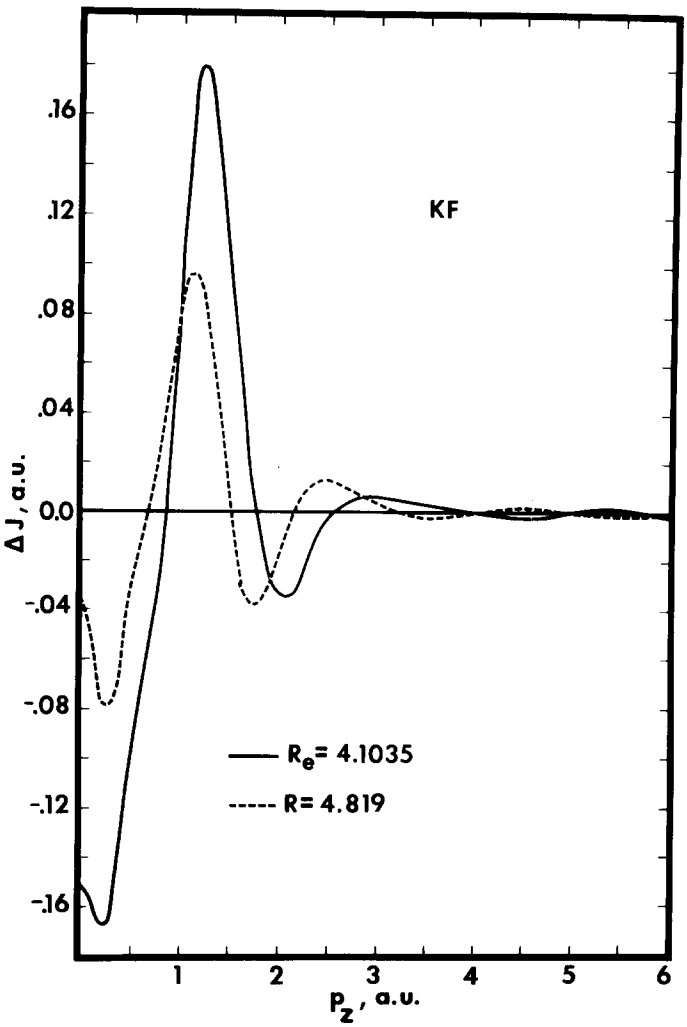

FIG. 10. Total Compton profile anisotropies for KF at several spacings.

sider, for example, NaF. The negative difference Δ for the $5\sigma^2(2s_F)$ MO, −0.0380, added to the positive differences from the $3\sigma^2(2s_{Na})$, $4\sigma^2(2p_{Na})$ and $6\sigma^2(2p_F)$ MO's, 0.0048, 0.0045, and 0.0346, respectively, sum to 0.0091. The magnitude of Δ for the $5\sigma^2$ MO derives primarily from a decrease in $J_0^{4\sigma}(0)$ since $J_{90}^{4\sigma}(0)$ is relatively constant for the two values of R. Decreasing R increases the polarization of the $2s_F$ orbital. This is manifested in increasing $p\sigma$ and $d\sigma$ bonding character for the $5\sigma^2$ MO. Since parallel $p\sigma$ profiles have zero components at $p_z=0$ while perpendicular profiles are maximum at this point (see for example $J^{4\sigma}(0)$ in Figs. 1 and 2) and since both s and $d\sigma$ profiles have non vanishing parallel and perpendicular components, the observed trends are not too surprising. It should be noted however that increasing $p\sigma$ character does not guarantee that $J_0(0)$ will decrease. To illustrate, increased polarization of the $2s_{Na}$ AO with decreasing R results in an increase in $J_0^{3\sigma}$ from 0.7806 to 0.7863. The main difference between the 3σ and 5σ results is that polarization of the $2s_F$ AO by the positive sodium ion increases charge in the bonding region while polarization of the $2s_{Na}$ AO by the negative fluoride ion decreases charge in this region. These effects can be substantial. The potassium fluoride $2s_F$ zero point profile, $J_0^{6\sigma}(0)$, decreases by 0.1174 with decreasing R while the $3s_K$ profile, $J_0^{5\sigma}(0)$, increased by 0.0518.

Regarding the second fact, that the variation of $\Delta J(0)$ with R is governed by changes in the valence pi orbital the variation in $J^{v\pi}(0)$ with R for LiF, NaF, and KF is −0.0084, 0.0669, and 0.0590, respectively. The corresponding variation in $\Delta J(0)$ for these three molecules is 0.0004, 0.0613, and 0.0833. These values are correlated. Polarization of the valence pi $(2p_F^{\pi})$ orbitals is manifested in increased $d\pi$ bonding character of the MO. The profiles $J_0^{d\pi}$ have zero component at $p_z=0$. Conversely $J_{90}^{d\pi}$ profiles are maximum at this point. Thus increasing $d\pi$ character with decreasing R results in a decreasing $J_0^{v\pi}(0)$ and relatively constant $J_{90}^{v\pi}(0)$.

Thus in both alkali fluorides and chlorides the valence pi orbital plays a significant role in determining both the general shape and R dependence of the anisotropy curves particularly in the low momenta region.

ACKNOWLEDGMENTS

The authors wish to acknowledge the support of the Robert A. Welch Foundation through grant no. E-397, the University of Houston Computing Center for generous amounts of computer time, and the UHCC Energy Foundation.

[1]R. L. Matcha, J. Chem. Phys. **47**, 5295 (1967); **49**, 1264 (1968); **53**, 4490 (1970); A. D. McLean, J. Chem. Phys. **39**, 2653 (1963).

[2]B. I. Ramirez, W. R. McIntire, and R. L. Matcha, J. Chem. Phys. **65**, 906 (1976).

[3]The primary atomic character of a particular MO is indicated in parenthesis. These are tabulated in col. 2 of Tables V–VIII for each alkali fluoride.

[4]T. Paakkari, E-L. Kohonen, O. Aikala, K. Mansikka, and S. Mikkola, Phys. Fenn. **9**, 207 (1974).

[5]R. L. Matcha, B. M. Pettitt, B. I. Ramirez, and W. R. McIntire, "Theoretical Compton Profile Anisotropies in Molecules and Solids. III Relationship Parallel–Perpendicular Anisotropies to Charge Distributions in Alkali Chloride Molecules," J. Chem. Phys. **69**, 3025 (1978).